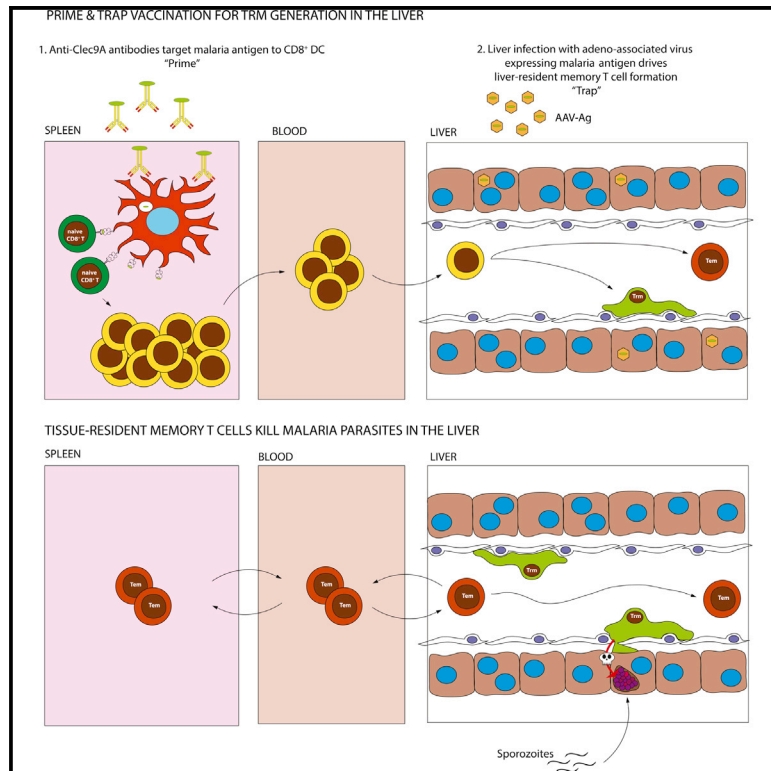


Immunity

Liver-Resident Memory CD8⁺ T Cells Form a Front-Line Defense against Malaria Liver-Stage Infection

Graphical Abstract



Authors

Daniel Fernandez-Ruiz, Wei Yi Ng, Lauren E. Holz, ..., Geoffrey I. McFadden, Irina Caminschi, William R. Heath

Correspondence

irina.caminschi@monash.edu.au (I.C.), wrheath@unimelb.edu.au (W.R.H.)

In Brief

While various intervention strategies have reduced morbidity and mortality from malaria, further improvement is likely to depend on an effective vaccine. Fernandez-Ruiz et al. identify liver-resident memory CD8⁺ T cells as vital for liver-stage immunity and describe a protective vaccination strategy that drives their formation.

Highlights

- CD8⁺ tissue-resident memory T cells (Trm cells) can be found in the murine liver
- These liver Trm cells survey the liver from within the sinusoids
- A prime-and-trap vaccination strategy efficiently induces liver Trm cells
- Liver Trm cells are essential for protection against liver-stage malaria after vaccination

Accession Numbers

GSE71518

Liver-Resident Memory CD8⁺ T Cells Form a Front-Line Defense against Malaria Liver-Stage Infection

Daniel Fernandez-Ruiz,¹ Wei Yi Ng,^{1,2} Lauren E. Holz,^{1,4} Joel Z. Ma,¹ Ali Zaid,^{1,4} Yik Chun Wong,⁶ Lei Shong Lau,¹ Vanessa Mollard,³ Anton Cozijnsen,³ Nicholas Collins,¹ Jessica Li,^{1,2} Gayle M. Davey,^{1,4} Yu Kato,¹ Sapna Devi,^{1,4} Roghieh Skandari,⁵ Michael Pauley,⁵ Jonathan H. Manton,⁵ Dale I. Godfrey,^{1,4} Asolina Braun,¹ Szun Szun Tay,⁶ Peck Szee Tan,^{2,8} David G. Bowen,⁶ Friedrich Koch-Nolte,⁷ Björn Rissiek,⁷ Francis R. Carbone,¹ Brendan S. Crabb,² Mireille Lahoud,^{2,8} Ian A. Cockburn,⁹ Scott N. Mueller,^{1,4} Patrick Bertolino,⁶ Geoffrey I. McFadden,³ Irina Caminschi,^{2,8,10,*} and William R. Heath^{1,4,10,*}

¹Department of Microbiology and Immunology, The Peter Doherty Institute, University of Melbourne, Parkville, VIC 3010, Australia

²Macfarlane Burnet Institute for Medical Research & Public Health, Melbourne, VIC 3004, Australia

³The School of BioSciences, University of Melbourne, Parkville, VIC 3010, Australia

⁴The ARC Centre of Excellence in Advanced Molecular Imaging, University of Melbourne, Parkville, VIC 3010, Australia

⁵Department of Electrical and Electronic Engineering, The University of Melbourne, Parkville, VIC 3010, Australia

⁶Liver Immunology Program, Centenary Institute and AW Morrow Gastroenterology and Liver Centre, University of Sydney and Royal Prince Alfred Hospital, Locked Bag No 6, Sydney, NSW 2042, Australia

⁷Institute of Immunology, University Medical Centre Hamburg-Eppendorf, Martinistrasse 52, 20246 Hamburg, Germany

⁸Infection and Immunity Program, Monash Biomedicine Discovery Institute and Department of Biochemistry and Molecular Biology, Monash University, Clayton, VIC 3168, Australia

⁹Department of Immunology and Infectious Disease, John Curtin School of Medical Research, Australian National University, Canberra, ACT 2601, Australia

¹⁰Lead contact

*Correspondence: irina.caminschi@monash.edu.au (I.C.), wrheath@unimelb.edu.au (W.R.H.)

<http://dx.doi.org/10.1016/j.immuni.2016.08.011>

SUMMARY

In recent years, various intervention strategies have reduced malaria morbidity and mortality, but further improvements probably depend upon development of a broadly protective vaccine. To better understand immune requirement for protection, we examined liver-stage immunity after vaccination with irradiated sporozoites, an effective though logistically difficult vaccine. We identified a population of memory CD8⁺ T cells that expressed the gene signature of tissue-resident memory T (Trm) cells and remained permanently within the liver, where they patrolled the sinusoids. Exploring the requirements for liver Trm cell induction, we showed that by combining dendritic cell-targeted priming with liver inflammation and antigen recognition on hepatocytes, high frequencies of Trm cells could be induced and these cells were essential for protection against malaria sporozoite challenge. Our study highlights the immune potential of liver Trm cells and provides approaches for their selective transfer, expansion, or depletion, which may be harnessed to control liver infections or autoimmunity.

INTRODUCTION

Plasmodium parasites have a complex life cycle involving several stages in both mosquito and mammalian hosts. During

a blood meal, sporozoites are released into the skin, where they access the blood and travel to the liver for the first stage of replication in their mammalian host. Halting parasite growth within the liver prevents progression to the subsequent disease-causing erythrocytic stage of infection. Numerous vaccination strategies have been tested for protection against pre-erythrocytic stages, with some showing promise in clinical trials (RTS,S Clinical Trials Partnership, 2014; Seder et al., 2013; European Medicines Agency, 2015). While targeting the pre-erythrocytic stages of *Plasmodium* development is by far the most clinically validated path to malaria vaccination, the approaches tested to date, including RTS,S, are far from optimal. One of the most clinically effective candidate vaccines uses radiation-attenuated sporozoites (RAS) produced in aseptic mosquitos (Seder et al., 2013), but this strategy suffers somewhat from logistical difficulties including scale and frequency of antigen dose and the route of administration. Identifying the basis of immune protection evoked by this vaccine, however, may allow development of more efficacious approaches.

The ability of RAS to protect against malaria was first demonstrated in mice (Nussenzweig et al., 1967) and has been shown to require CD8⁺ T cells (Weiss et al., 1988), although some contribution by humoral immunity is likely (Rodrigues et al., 1993). Although very high numbers of circulating memory CD8⁺ T cells are required to maintain protection (Schmidt et al., 2008), several studies using RAS to vaccinate mice have identified memory CD8⁺ T cell populations within the liver that have unique properties that may benefit immunity (Berenzon et al., 2003; Epstein et al., 2011; Nganou-Makamdop et al., 2012; Tse et al., 2013). CD8⁺ T cell-mediated effector mechanisms responsible for protection in mice are not fully resolved, but

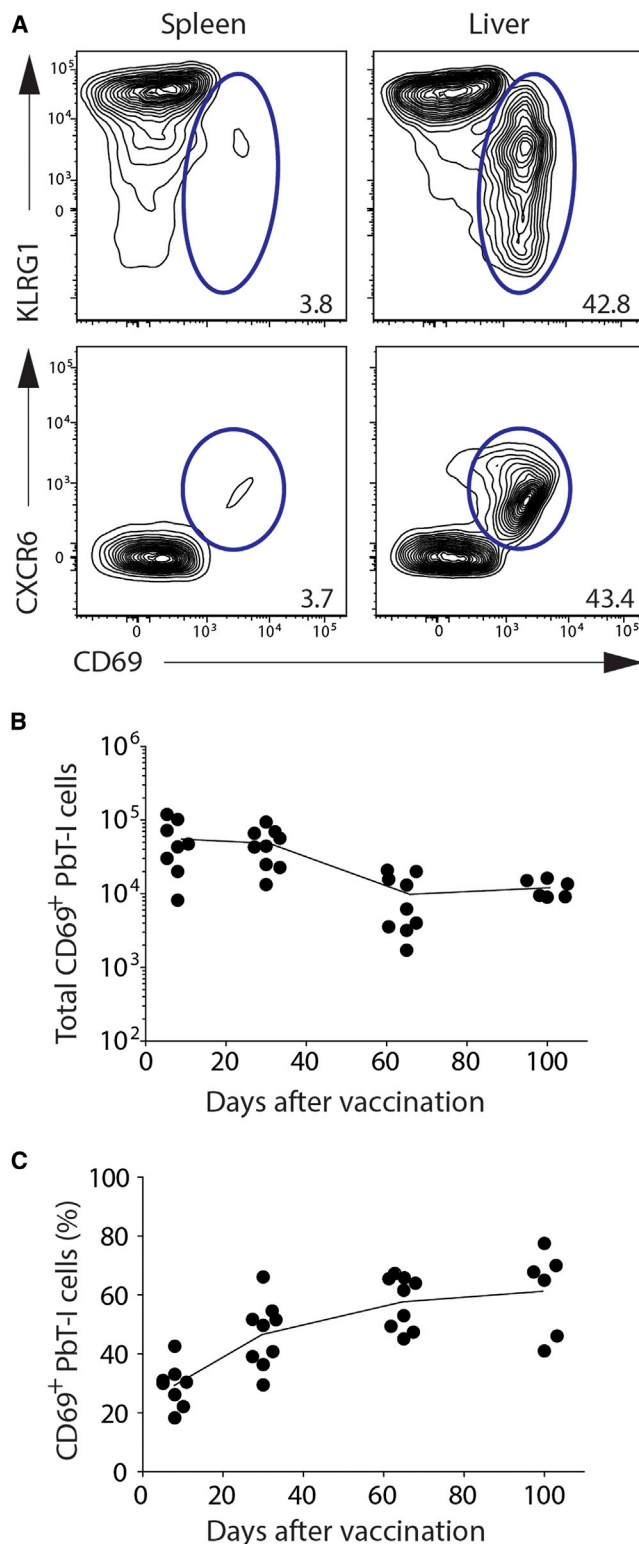


Figure 1. Identification of Liver-Associated Memory T Cells
 (A) Expression of surface markers by PbT-I cells in the spleen (left) and liver (right) after vaccination. B6 mice were transferred with 50,000 PbT-I cells expressing GFP (PbT-I.GFP) and then 1 day later vaccinated i.v. with 50,000 PbA RAS. 31 days later, spleens and livers were harvested and single cells stained for defined markers. After gating on GFP⁺CD44^{hi}CD8⁺ cells, expres-

cytotoxicity and effector molecules such as interferon- γ (IFN- γ) and tumor necrosis factor- α (TNF- α) make varying contributions depending on the species of *Plasmodium* tested (Butler et al., 2012).

The discovery of non-recirculating Trm cells within organs such as the skin and gut (Schenkel and Masopust, 2014) led to speculation that liver-resident memory T cells may be involved in protection against sporozoites (Tse et al., 2014), though residency per se was never established. This conclusion was based on high expression of CXCR6 by liver-associated memory CD8⁺ T cells after RAS vaccination (Tse et al., 2013) and a reduction of both liver-associated memory and sporozoite immunity when T cells lack this receptor (Tse et al., 2014). Imaging studies reveal CD8⁺ T cells (of undefined specificity) showing high motility within the liver sinusoids of immune hosts, suggesting that memory T cells survey for liver infection by patrolling the sinusoids (Cabrera et al., 2013). More recently, resident populations of CD8⁺ T cells have been identified in the liver after LCMV infection (Steinert et al., 2015). How these liver-resident populations are formed in response to this systemic infection and whether they represent the same types of T cells associated with malaria liver-stage immunity (Tse et al., 2014) is, however, unclear. Thus, although liver-associated T cells have been implicated in malaria immunity after RAS vaccination, their residence status and location are poorly defined.

Here, we have undertaken a detailed assessment of liver-associated memory CD8⁺ T cells generated by vaccination with the “gold-standard” malaria liver-stage vaccine, RAS. We identified a population of CD8⁺ T cells that patrol the liver sinusoids and reside permanently within the liver. We show that this liver-resident population can also be generated by a “prime-and-trap” vaccination strategy and that such liver-resident T cells can be harnessed for protection against sporozoite challenge.

RESULTS

Immunization with RAS Induces Liver-Resident Memory CD8⁺ T Cells

To examine CD8⁺ T cell immunity induced by RAS vaccination, we transferred 50,000 GFP⁺CD8⁺ T cells from the PbT-I T cell receptor transgenic mouse (specific for a malaria antigen expressed by both sporozoites and blood-stage parasites) (Lau et al., 2014) into wild-type B6 mice that were then vaccinated with 50,000 *P. berghei* ANKA (PbA) RAS. 31 days later, we assessed the phenotype of PbT-I CD8⁺ T cells in the liver and spleen. Based on expression of CD69 and KLRG1 or CXCR6, two distinct T cell populations were evident in the liver, but only one of these was found in the spleen (Figure 1A). The vast

sion of CD69 versus KLRG1 or CXCR6 was examined. Representative flow cytometry profiles for four mice in two independent experiments are shown with percent indicated for oval gates.

(B and C) Quantitation of CD69⁺ PbT-I cells in the liver after vaccination with RAS. Experimental approach as in (A), but CD44^{hi} PbT-I.GFP cells were examined for CD69 and CD62L expression at multiple time points after vaccination to identify the number (B) and proportion (C) of CD69⁺CD62L⁻ cells. Each point represents a mouse. Data pooled from two independent experiments for each time point; lines join the means.

Please see Figure S1.

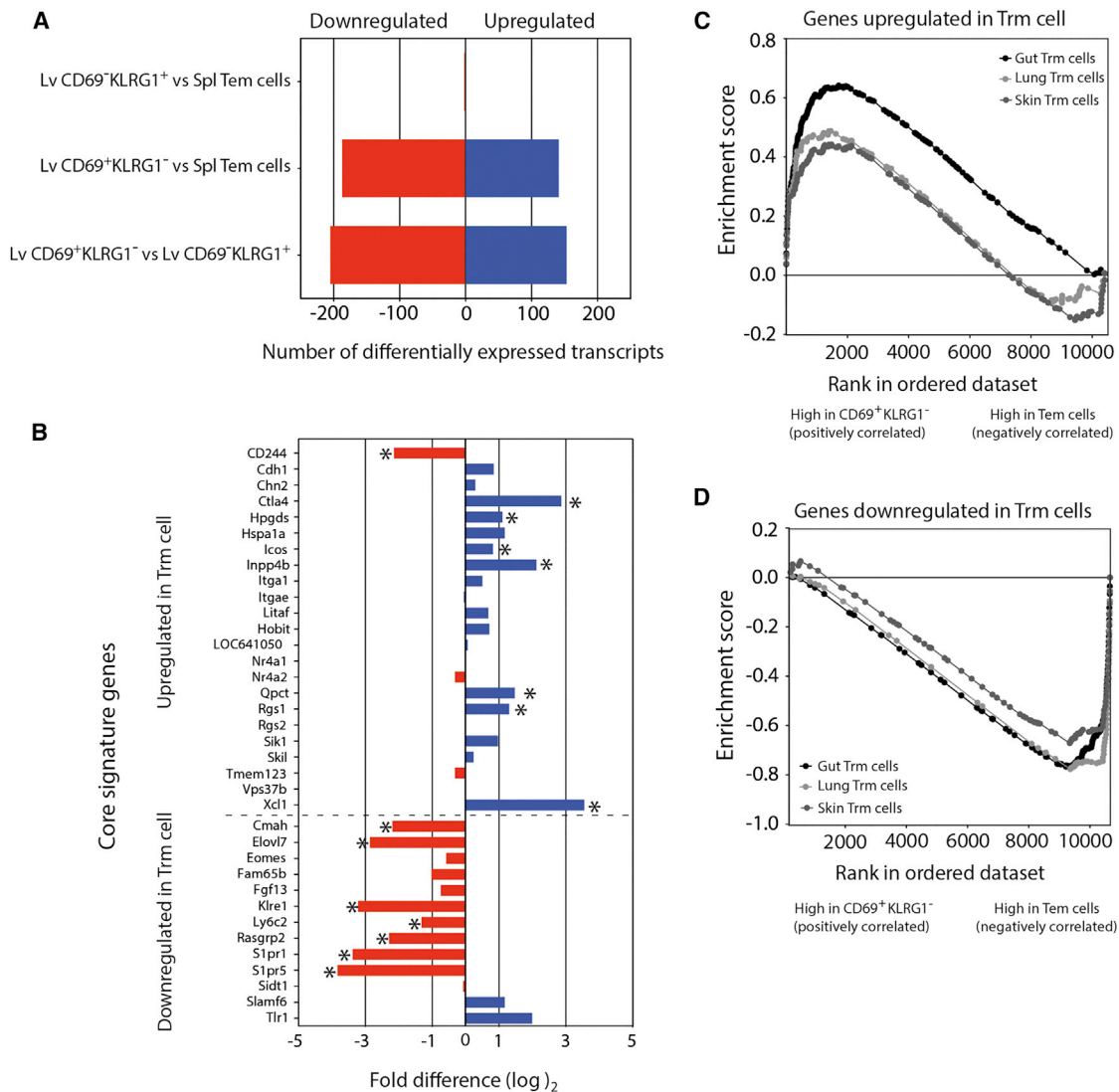


Figure 2. Differential Gene Expression by Memory T Cells in the Liver and Spleen

50,000 PbT-I.GFP cells were transferred into B6 mice that were then vaccinated with 50,000 RAS. 29 days after vaccination, memory GFP⁺CD44^{hi}CD8⁺ PbT-I cells were sorted from the spleen (CD69⁻CD62L⁻ Tem cells) and liver (either CD69⁻KLRG1^{lo} or CD69⁻KLRG1^{hi}) and examined for gene expression by microarray analysis.

(A) Number of differentially expressed genes ($\geq \log_2$ -fold; satisfying the Benjamini and Hochberg adjusted p value of < 0.05) by splenic Tem cells and liver T cell populations.

(B) Fold change expression of Trm cell core signature genes (Mackay et al., 2013) in CD69⁻KLRG1^{lo} T cells relative to liver Tem cells (CD69⁻KLRG1^{hi}). *Benjamini and Hochberg adjusted p value < 0.05 .

(C and D) Enrichment score of upregulated (C) or downregulated (D) gene sets from gut, lung, or skin Trm cells (Mackay et al., 2013) in liver CD69⁻KLRG1^{lo} T cells relative to liver Tem cells (CD69⁻KLRG1^{hi}). False discovery rate q value (FDR) of the enrichment scores (ESs) of upregulated expression gene sets from gut, lung, and skin Trm cells in liver Trm cells was 0.0000, 0.0003, and 0.0006, respectively. ES FDR of downregulated expression gene sets from gut, lung, and skin Trm cells in liver Trm cells were all 0.0000. ESs were considered significant when FDR < 0.05 . All data were derived from a single experiment.

Please see Table S1 and Figure S2.

majority of KLRG1⁺CD69⁻ cells in the spleen were CD62L⁻ (not shown), identifying them as either effectors or effector memory T cells (Tem). Given the long-term persistence of this population (Figure S1), we will simply refer to them as Tem cells. PbT-I cells expressing CD69, a marker of Trm cells in other tissues (Schenkel and Masopust, 2014), were maintained in the liver for >100 days (Figure 1B) and represented $\sim 60\%$ of intrahepatic

PbT-I T cells (Figure 1C), suggesting that they were also long-lived. Microarray analysis of gene expression showed that PbT-I Tem cells in the spleen had virtually identical gene expression profiles to CD69⁻KLRG1^{hi} cells in the liver (Figure 2A and Table S1), indicating that these two populations were identical and most likely recirculating Tem cells. By examining the gene expression differences between these Tem cells and the

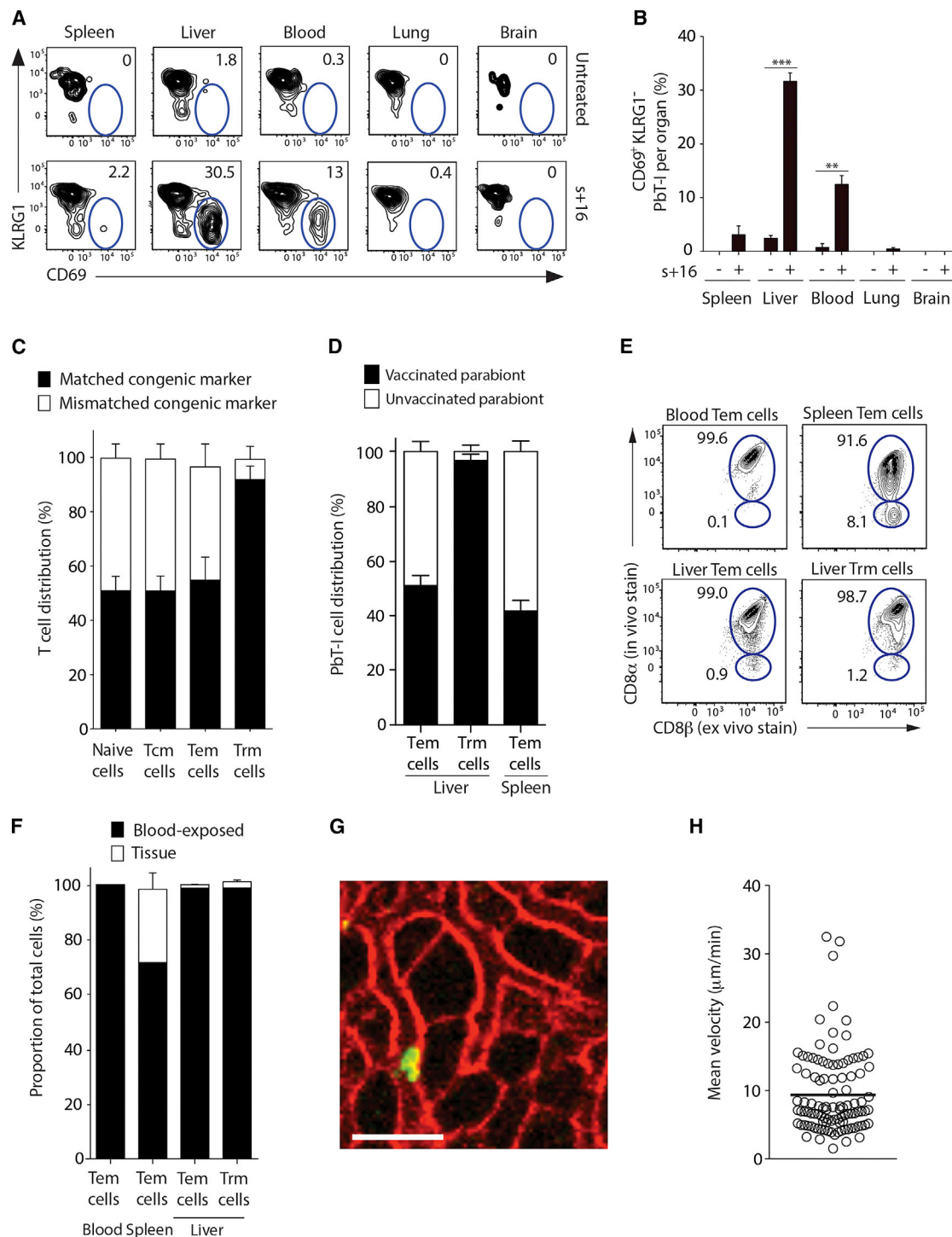


Figure 3. Homing and Recirculation Pattern of Liver Trm Cells

(A and B) Blocking of ARTC2.2 shows that Trm cells home to the liver. Memory PbT-I.GFP cells were derived from the livers of male mice 35–36 days after vaccination with 50,000 RAS. Donor mice were either left untreated (top) or given s+16 αARTC2.2 nanobody (bottom) 15 min before isolation of liver PbT-I cells for adoptive transfer into naive recipients. 3 days later, recipient tissues were examined for the presence of PbT-I.GFP cells.

(A) Representative profiles of PbT-I.GFP cells harvested from each organ, showing oval gates and percentages for regions containing Trm cells.

(B) Proportion of PbT-I.GFP Trm cells (CD69⁺KLRG1⁺) within each tissue for pooled data from two independent experiments; four mice given treated cells and three mice given untreated cells. A significantly higher proportion of treated Trm cells were found in the blood and liver ($p = 0.0022$; $p < 0.0001$; unpaired t test). Means and SEM are shown.

(legend continued on next page)

CD69⁺KLRG1^{lo} liver population (Figures 2A and 2B and Table S1), many genes represented in the core gene signature of lung, skin, and gut Trm cells (Mackay et al., 2013) were similarly up- or downregulated in liver CD69⁺KLRG1^{lo} T cells (now simply referred to as liver Trm cells), though a number of these differences did not reach statistical significance (Figure 2B). Gene-set enrichment analysis of liver Trm cells also showed strong similarity to Trm cells from gut, skin, and lung (Figures 2C and 2D). Together, these data suggested that vaccination with RAS induced a memory T cell population exhibiting Trm cell gene expression in the liver.

To phenotype liver Trm cells in detail, we examined expression of a panel of surface proteins, some based on differential gene expression (Table S1). Figure S2 shows that liver Trm cells lacked CD103 expression and differentially expressed CXCR3, CXCR6, CD101, BTLA, FR4, Ly6ae, CD25, CD31, CD93, IL-4R, CD127, gp130, CD200R, and CD43, whereas Tem cells differentially expressed KLRG1, CX3CR1, and NKG2D.

To assess whether liver Trm cells homed to the liver, we transferred PbT-I cells from the livers of immune mice into naive mice and assessed homing after 3 days. Only Tem phenotype cells could be recovered, however, suggesting that Trm cells died upon transfer (Figure 3A, top). Liver NKT cells also fail to survive adoptive transfer unless their cell-surface enzyme ARTC2.2 is blocked (Rissiek et al., 2014). ARTC2.2 uses NAD⁺ (probably released during the liver preparation) to ADP-ribosylate adjacent cell-surface P2X7 receptors, opening this ion channel and causing cell death (Seman et al., 2003). Because liver Trm cells expressed high amounts of RNA for the corresponding *Art2b* and *P2rx7* genes (Table S1), we assessed whether treating vaccinated mice with the nanobody s+16a, which blocks ARTC2.2 function, would enable transfer and survival of liver Trm cells. This was the case, as shown by the fact that liver Trm cells survived transfer and preferentially homed to the liver, but not brain, lungs, or spleen (Figures 3A, bottom, and 3B).

To verify the “resident” status of liver Trm cells, we used parabiosis. Naive mice contained a population of endogenous Trm cells (Figure S3), so we simply parabiosed naive Ly5.1 and Ly5.2 B6 mice and assessed the Ly5 phenotype of liver T cells 14–17 days later (Figure 3C). This showed full mixing of naive, Tem, and central memory T (Tcm) cells, indicating that these cells recirculated between parabiotic partners. Very little mixing

of liver Trm cells, however, suggested that these cells were resident. We also examined recirculation of T cells in parabiotic mice where one partner had been transferred with PbT-I cells and immunized with RAS (Figure 3D). Lack of recirculation of PbT-I liver Trm cells between parabiotic partners confirmed their liver-resident status, while exchange of PbT-I Tem cells indicated their capacity for recirculation. Together, protein and gene expression profiles, homing capacity, and parabiosis studies strongly indicate that RAS vaccination induces a liver-resident population of memory CD8⁺ T cells.

Liver Trm Cells Patrol the Liver Sinusoids

Trm cells can be located within tissue epithelia or the central nervous system, having minimal access to the blood (Schenkel and Masopust, 2014). This is not universal, however; tissue-resident T cells of the spleen, liver, and kidney may be located within the circulatory architecture (Geissmann et al., 2005; Schenkel and Masopust, 2014; Steinert et al., 2015; Thomas et al., 2011). To identify the location of malaria-specific liver Trm cells, we used a technique described by Galkina et al. (2005) where α -CD8 mAb is injected prior to cell harvesting to selectively label cells within the blood. This showed that virtually all PbT-I memory CD8⁺ T cells in the liver were blood exposed (Figures 3E and 3F). However, endothelium of the liver is fenestrated, allowing rapid leakage of Ab into the tissue, potentially causing labeling of T cells located outside the sinusoids. To verify that malaria-specific memory T cells were located within the circulation, we used intravital multiphoton microscopy to visualize GFP-expressing PbT-I cells in the liver of RAS-vaccinated mice (Figure 3G and Movies S1 and S2). This revealed that PbT-I cells were located largely within the liver sinusoids, migrating at \sim 10 μ m per min (Figure 3H). Many PbT-I cells showed an amoeboid shape and migration pattern akin to patrolling the sinusoid. Some appeared more rounded and essentially flowed in the blood, occasionally stopping within vessels. This latter group probably represented circulating Tem cells. Further, more detailed, phenotypic analyses of T cell migration patterns within the liver are provided later using an alternative vaccination approach. Given the fenestrated nature of liver sinusoidal endothelium, the close associations of sinusoids with hepatocytes, and the capacity of sinusoidal T cells to interact with hepatocytes (Guidotti et al., 2015; Warren et al., 2006), the migration pattern

(C) Recirculation of endogenous CD8⁺ T cells in parabiotic mice. Ly5.1 and Ly5.2 B6 mice were maintained in parabiosis for 14–17 days before testing Ly5.1 and Ly5.2 expression by liver CD8⁺ T cells. Shown is the percent of parental cells (black bars) or partner cells (white bars) for each parabiotic. T cells include CD44^{lo} naive (Naive), CD44^{hi}CD62L⁺CD69⁻ Tcm, CD44^{hi}CD62L⁻CD69⁻ Tem, and CD44^{hi}CD62L⁻CD69⁺ Trm cells. Data from two independent experiments with one or two parabiotic pairs for a total of six mice. Means and SEM are shown. For phenotype of liver T cells in naive mice, see Figure S3.

(D) Recirculation of memory PbT-I cells in parabiotic mice. B6 mice were given 50,000 naive PbT-I.GFP cells, vaccinated with 50,000 RAS, and then 35 days later joined by parabiosis to naive B6 mice. 30 days later, the distribution of PbT-I cells in the vaccinated (black bars) or unvaccinated (white bars) partners was assessed. Data from one experiment with three parabiotic pairs. Means and SEM are shown.

(E and F) Location of memory CD8⁺ T cells in the liver. B6 mice received 50,000 PbT-I.GFP cells and were injected with 25,000–50,000 RAS. 27–30 days later, mice were injected i.v. with α -CD8 α Ab and then sacrificed 5 min later. Cells from different organs were then stained with an α -CD8 β ex vivo to distinguish blood-exposed from tissue-associated CD8⁺ T cells.

(E) Representative profiles of PbT-I.GFP cells for different organs. Upper oval gates define blood-exposed cells, whereas lower oval gates denote other cells.

(F) Quantitation of blood-exposed (black bars) and non-exposed (white bars) PbT-I.GFP cells. Data pooled from two independent experiments with seven mice total. Mean and SEM are shown.

(G) Single frame from intravital imaging of GFP⁺ PbT-I cells within the liver of RAS-vaccinated TdTomato mice that ubiquitously express a membrane form of TdTomato. Mice were vaccinated with RAS 30 days prior to imaging. Scale bar represents 30 μ m.

(H) Mean velocity of individual PbT-I cells from mice vaccinated as in (G). Six movies from three mice were analyzed.

Please see Movies S1 and S2.

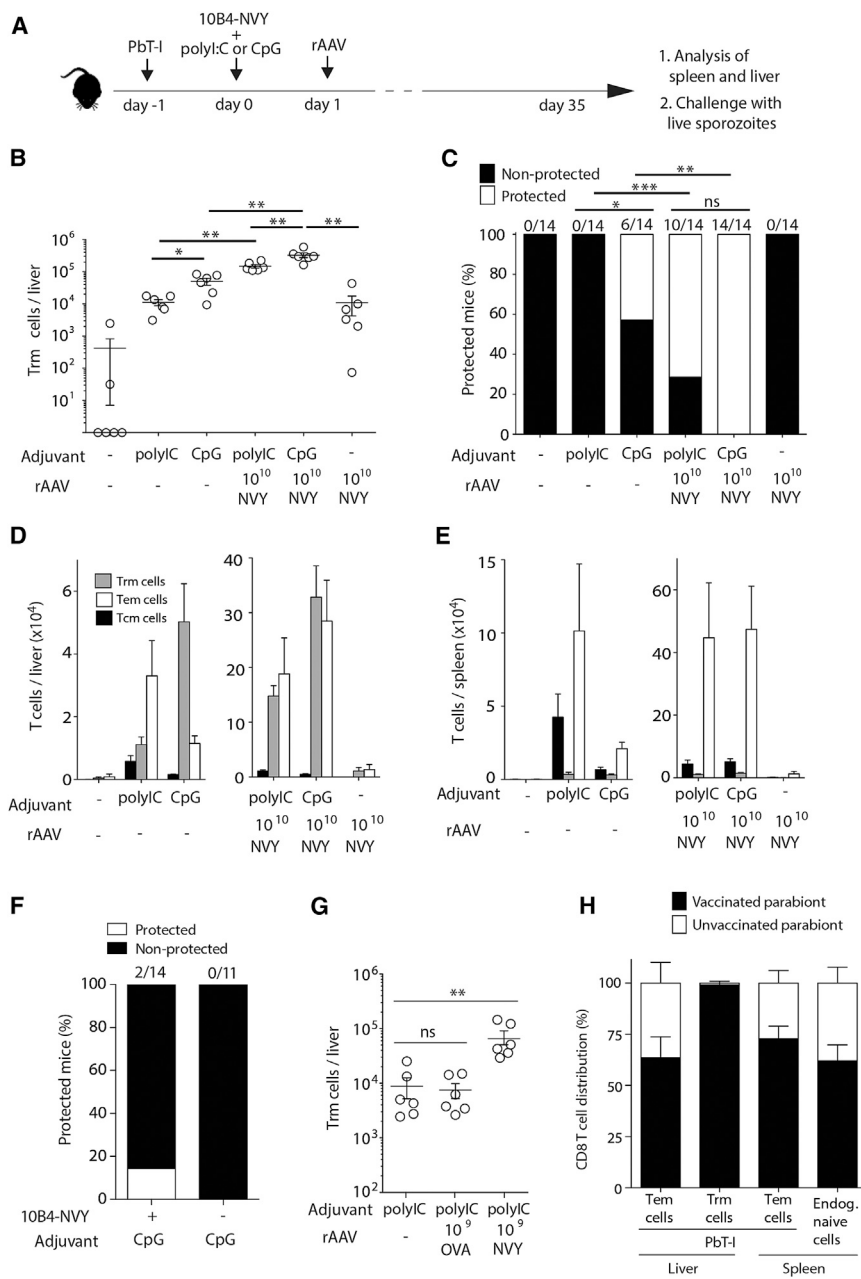


Figure 4. Prime-and-Trap Immunization Induced Liver Trm Cells that Protect against Sporozoite Infection

(A) Vaccination scheme.

(B and C) B6 mice were injected with 50,000 PbT-I.GFP CD8⁺ T cells and the next day vaccinated i.v. with 8 μg α-Clec9A-NVY alone or together with poly(I:C) or CpG. 1 day later, mice were either left untreated or vaccinated i.v. with 10¹⁰ vgc of rAAV-NVY. One group received only rAAV-NVY with no anti-Clec9A-NVY. Mice were (B) assessed for PbT-I liver Trm cell numbers on day 34–36 after vaccination (*p < 0.05; **p < 0.01; ns, not significant; two-tailed Mann-Whitney test) or (C) challenged with 200 PbA sporozoites on day 35 after vaccination and assessed for protection based on break-through blood-stage parasitemia. Numbers above bars represent protected mice over total mice (*p < 0.05; **p < 0.01; ***p < 0.001; ns, not significant; Fisher's exact test). Pooled data from two independent experiments. Individual mice and mean and SEM are shown in (B).

(D and E) Histograms showing number of each memory PbT-I cell subset recovered from (D) the liver and (E) the spleen of mice from (B). CD8⁺ T cells were identified as Tcm cells (CD44⁺CD62L⁺CD69⁻), Tem cells (CD44⁺CD62L⁻CD69⁻), or Trm cells (CD44⁺CD62L⁻CD69⁺). Mean and SEM are shown.

(F) CpG adjuvant alone does not protect mice against sporozoite infection. B6 mice received 50,000 PbT-I.GFP cells and 1 day later were injected with either 8 μg anti-Clec9A-NVY (10B4-NVY) and CpG or with CpG adjuvant alone. Protection against infection with 200 PbA sporozoites was assessed on day 35–49. Numbers above bars represent protected mice over total mice. Data pooled from two independent experiments. Mean and SEM are shown.

(G) Specific antigen expression in the liver is required for augmented Trm cell formation by rAAV. Mice received 50,000 PbT-I.GFP cells and 1 day later were primed with 8 μg anti-Clec9A-NVY combined with poly(I:C). One day later, mice were left untreated or received 10⁹ rAAV expressing either the SIINFEKL peptide from ovalbumin (rAAV-OVA) or the NVY peptide recognized by PbT-I cells (rAAV-NVY). Total liver Trm cell numbers were determined on days 22–23 after infection. (**p < 0.01; ns, not significant; two-tailed Mann-Whitney test.)

(H) Recirculation of memory PbT-I cells in parabolic mice. Mice vaccinated by prime-and-trap as in (A), using CpG as adjuvant, were joined to naive mice 30 days after priming and maintained as parabolic mice for 14 days before examining the presence of PbT-I cells in each partner. Shown is the distribution of CD8⁺ T cells (either PbT-I or naive endogenous CD8 T cells) in the vaccinated (black) or unvaccinated (white) partners. T cell populations included CD44^{hi}CD62L⁻CD69⁻ PbT-I Tem cells, CD44^{hi}CD62L⁻CD69⁺ PbT-I Trm cells, and CD44^{lo} naive endogenous CD8⁺ T cells. Data from two independent experiments with a total of four parabolic pairs. Means and SEM are shown.

of patrolling T cells within the sinusoids represents an ideal pattern for surveillance of hepatocyte infection.

A Prime-and-Trap Strategy Is Capable of Expanding Liver Trm Cells and Protecting against Sporozoite Challenge

Because vaccination with RAS induces liver Trm cells (Figure 1) and protects against sporozoite challenge (Epstein et al., 2011),

we hypothesized that developing a vaccination strategy that maximized liver Trm cell numbers would be protective. To test this hypothesis, we designed a two-staged vaccine (Figure 4A) that first activated T cells in the spleen and then trapped them in the liver, to form Trm cells. For the first stage, we sought to efficiently prime malaria-specific CD8⁺ T cells. Because i.v. vaccination with RAS relies upon antigen presentation by splenic CD8α⁺ dendritic cells (DCs) (Lau et al.,

2014), we delivered our peptide antigen to CD8 α ⁺ DCs conjugated to a mAb that targets the surface receptor Clec9A, expressed by this DC subset. Because CD8⁺ T cell priming by Clec9A-targeted antigen requires adjuvant (Lahoud et al., 2011), we combined this with either poly(I:C), a toll-like receptor-3 (TLR3) agonist, or CpG, a TLR9 agonist. The second stage of our strategy involved expressing antigen on hepatocytes to trap circulating primed CD8⁺ T cells in the liver, facilitating conversion to Trm cells. This was loosely based on the observation that T cells in the brain convert to CD103⁺ Trm cells upon antigen encounter (Wakim et al., 2010) and is akin to the “prime-and-pull” approaches that use chemokines (Shin and Iwasaki, 2012) or inflammation (Mackay et al., 2012) to attract T cells to specific sites for Trm cell formation. Hepatocyte expression of antigen was achieved by using a recombinant adeno-associated virus (rAAV) that targets hepatocytes and expresses its antigenic cargo via the hepatocyte-specific α -1 antitrypsin promoter (Tay et al., 2014). To track malaria-specific T cells after vaccination, we seeded mice with 50,000 PbT-I T cells and then used the agonistic peptide epitope NVYDNFLL (NVY) linked to α Clec9A mAb or expressed in rAAV (rAAV-NVY) as our vaccine components. Analyses of liver and splenic PbT-I cells 34–36 days after vaccination, once viral antigen was cleared from the liver (Figure S4), revealed effects of both adjuvant and viral components on memory T cell formation (Figures 4B, 4D, and 4E). In the absence of the rAAV component, Clec9A-targeted priming with CpG was superior to poly(I:C) in forming liver Trm cells (Figures 4B and 4D, left graph). When such priming was combined with rAAV-NVY (and therefore hepatic antigen expression), a greater number of Trm cells were induced, with CpG again superior to poly(I:C) (Figures 4B and 4D, right graph). Challenge of these groups of mice with 200 sporozoites on day 35 after vaccination confirmed CpG to be a more effective adjuvant than poly(I:C) and revealed that in this experiment 100% of mice were protected against malaria when given the combined prime-and-trap vaccine with CpG and specific virus (Figure 4C). Protection in CpG-treated animals was not simply a consequence of exposure to this adjuvant because adjuvant alone (without Clec9A-targeted antigen) was not protective (Figure 4F). Formation of large numbers of liver Trm cells was, however, dependent on viral expression of specific antigen, since expression of an irrelevant antigen, e.g., ovalbumin (rAAV-OVA), did not enhance Trm cell formation (Figure 4G).

To establish that PbT-I Trm cells generated by prime-and-trap vaccination were liver resident, we generated parabiotic mice between naive B6 mice and vaccinated B6 mice seeded with PbT-I cells (Figure 4H). This confirmed that PbT-I Trm cells remained in the livers of immune hosts, whereas Tem cells migrated between partners.

Comparison of protection induced by immunization with RAS to that generated by the prime-and-trap vaccine showed RAS to be less effective despite their potential to induce an additional antibody component (Figure 5A). Greater protection by the prime-and-trap regime again correlated with higher numbers of liver Trm cells (Figure 5B). Intravital imaging of prime-and-trap vaccinated mice further confirmed efficient formation of liver-patrolling Trm cells within the sinusoids (Movies S3 and S4).

Liver Trm Cells Show a Distinct Migration Pattern Relative to Tem Cells

To better define the migration patterns of Tem and Trm cells in the liver, we took advantage of the observation that CXCR6 and CX3CR1 were expressed reciprocally by these cells (Figure S2). We crossed PbT-I mice to either *Cx3cr1*-GFP mice to express GFP in Tem cells or to *Cxcr6*-GFP mice to express GFP mainly in Trm cells (Figure 5C) and then examined the migration pattern of GFP-expressing cells in vaccinated mice (Figure 5D and Movies S5 and S6). Multiphoton microscopy revealed that Tem cells were rounded in shape and flowed rapidly in the sinusoids but occasionally stopped briefly, sticking in the sinusoids. In contrast, Trm cells appeared more amoeboid in shape and migrated with a crawling action (patrolling) along the sinusoids. Tem cells had a broad range of velocities, with most tracked cells moving slower than Trm cells, but tracking constraints meant that this analysis excluded cells present for <4 frames such as those flowing rapidly in the vessels (Figures 5E and 5F). Examination of circularity (Figures 5G and 5H), a 2-dimensional measure of roundness, confirmed that Tem cells were generally rounder than Trm cells, most likely because patrolling Trm cells crawled along the sinusoids, slightly stretching their cell bodies.

Protection by Prime-and-Trap Vaccination Depends on Trm Cells

Our findings indicated a significant correlation between protection and the number of Trm cells or Tem cells in the liver, though the correlation coefficient was higher for Trm cells (Figure 6A). To directly address the role of Trm cells in protection, we examined microarray data for specific markers to deplete Trm cells. One marker, CXCR3, was expressed by all liver Trm cells and was largely absent from Tem cells (Figure 6B). Injection of mAb to this marker into prime-and-trap vaccinated mice on days 32 and 34 after vaccination revealed almost complete depletion of liver Trm cells by flow cytometry (Figures 6C–6F) and a loss of cells of a patrolling phenotype by intravital imaging (Movie S7) with no significant loss of splenic or liver Tem cells (Figures 6C–6F). When similarly treated mice were challenged with 200 sporozoites on day 35 after vaccination, protection was completely lost in the mice depleted of Trm cells (Figure 6G), implicating these cells in protection. Consistent with this conclusion, protection was also lost after depleting mice of CD8⁺ cells (Figure 6H) but was not lost in CD1d-deficient mice, which lack NKT cells, another CXCR3⁺ liver cell type (Figure 6I), nor in mice depleted of a combination of CD4⁺ and NK1.1⁺ cells, which would include NKT and NK cells (Figure 6J). We also depleted CXCR3⁺ cells from mice immunized twice with RAS, which lost protection (Figure 6K) and showed a significant increase in parasitemia on day 6 (mean parasitemia in isotype-treated mice 0.08%; mean parasitemia in α -CXCR3-treated mice 0.95%; $p = 0.0001$, two-tailed Mann-Whitney test). These data support the conclusion that liver Trm cells are critical for protection after vaccination with prime-and-trap or RAS.

To compare effector molecule expression by Trm and Tem cells, PbT-I cells from mice vaccinated by prime-and-trap were examined for expression of IFN- γ , TNF- α , and granzyme B and the degranulation marker CD107a (Figures 7A–7F). Mice used in these experiments were injected with anti-ARTC2.2 nanobody

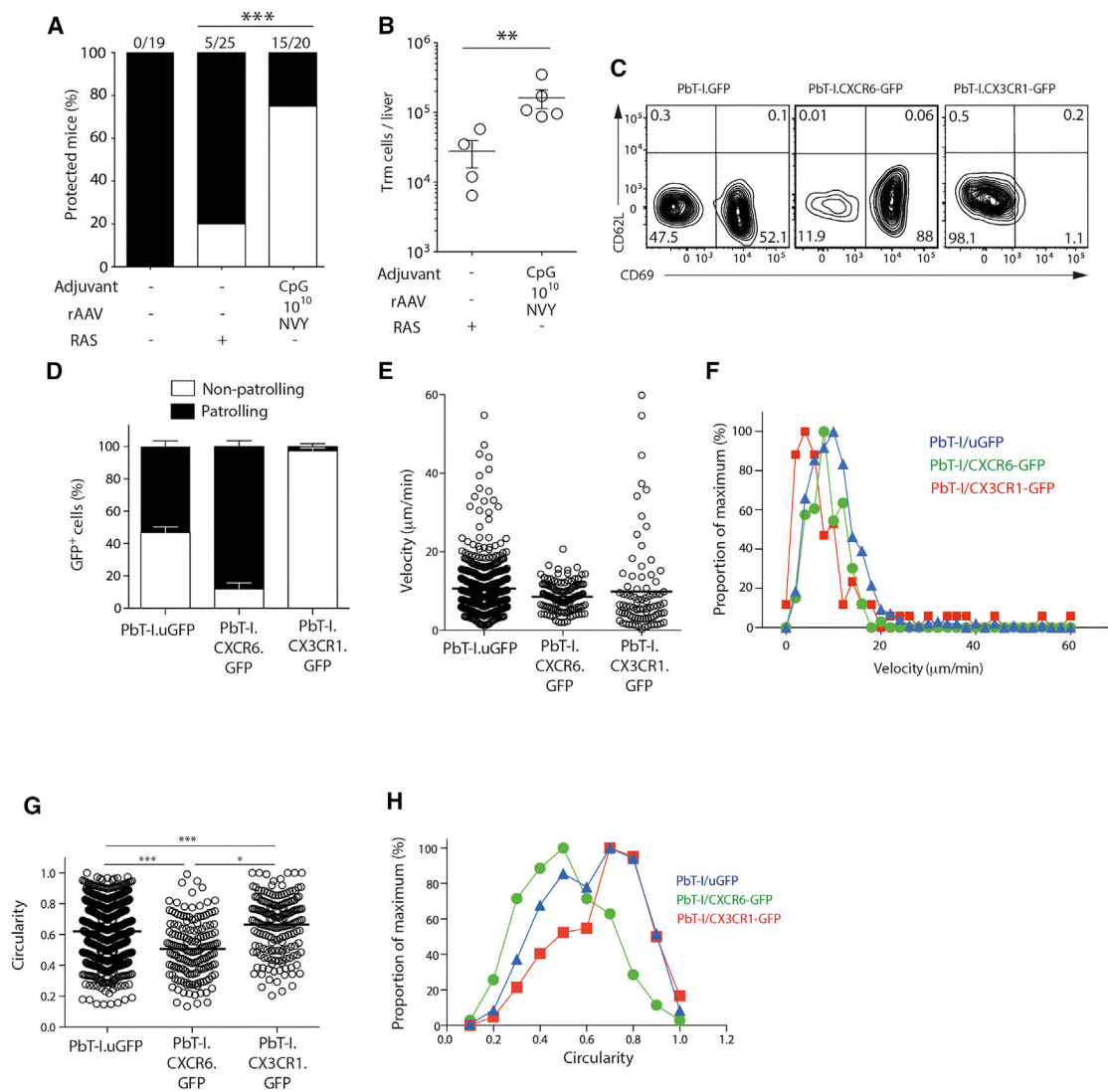


Figure 5. Protection and T Cell Migration Patterns after Prime-and-Trap Vaccination

(A and B) Mice received 50,000 PbT-I.uGFP cells and 1 day later were vaccinated with either 50,000 RAS or with 8 μg α-Clec9A-NVY with CpG followed the next day by 10¹⁰ rAAV-NVY. Data pooled from two independent experiments.

(A) 35 days later, mice were challenged with 200 sporozoites and protection determined by detection of breakthrough blood-stage parasites (**p < 0.0003, Fisher's exact test). Numbers above bars represent protected mice out of total mice.

(B) Numbers of liver Trm cells were determined on day 35–36 after priming. Data were log-transformed and analyzed with a two-tailed unpaired t test (**p = 0.0074).

(C–H) PbT-I mice were crossed to mice expressing GFP under the CX3CR1 promoter (PbT-I.Cx3cr1-GFP) or the CXCR6 promoter (PbT-I.Cxcr6-GFP) or a ubiquitous promoter (PbT-I.uGFP). 50,000 of these PbT-I cells were seeded into wild-type hosts that were then vaccinated by prime-and-trap.

(C) 35–39 days later, cells were harvested from the liver and GFP-expressing PbT-I cells examined for CD69 and CD62L. Each profile is from a different experiment.

(D) Intravital multiphoton movies from vaccinated mice were quantitated for cells showing patrolling (crawling) behavior (black) or non-patrolling behavior (flowing in blood, sticking in sinusoids without crawling) (white). Mean and SEM are shown.

(E and F) Velocity of GFP⁺ PbT-I cells from vaccinated mice for individual cells (E) or for cells binned in 2% increments of velocity (F).

(G and H) Circularity of GFP⁺ PbT-I cells from vaccinated mice for individual cells (G) or cells binned in 10% increments of circularity (H).

Data for (C)–(H) are from eight to nine mice per phenotype from two to three independent experiments. Please see [Movies S3, S4, S5, and S6](#).

15 min before harvesting liver T cells because, without treatment, Trm cells showed poor survival during the 6 hr in vitro re-stimulation (not shown). This analysis revealed greater effector function by Trm relative to Tem cells, consistent with Trm cells being the dominant mediators of protection.

Modeling Identifies the Relationship between Trm Cell Numbers and Liver Surveillance Time

To quantitatively predict requirements for control of liver-stage malaria by liver Trm cells, we have developed a mathematical model for liver surveillance, detailed in the [Supplemental](#)

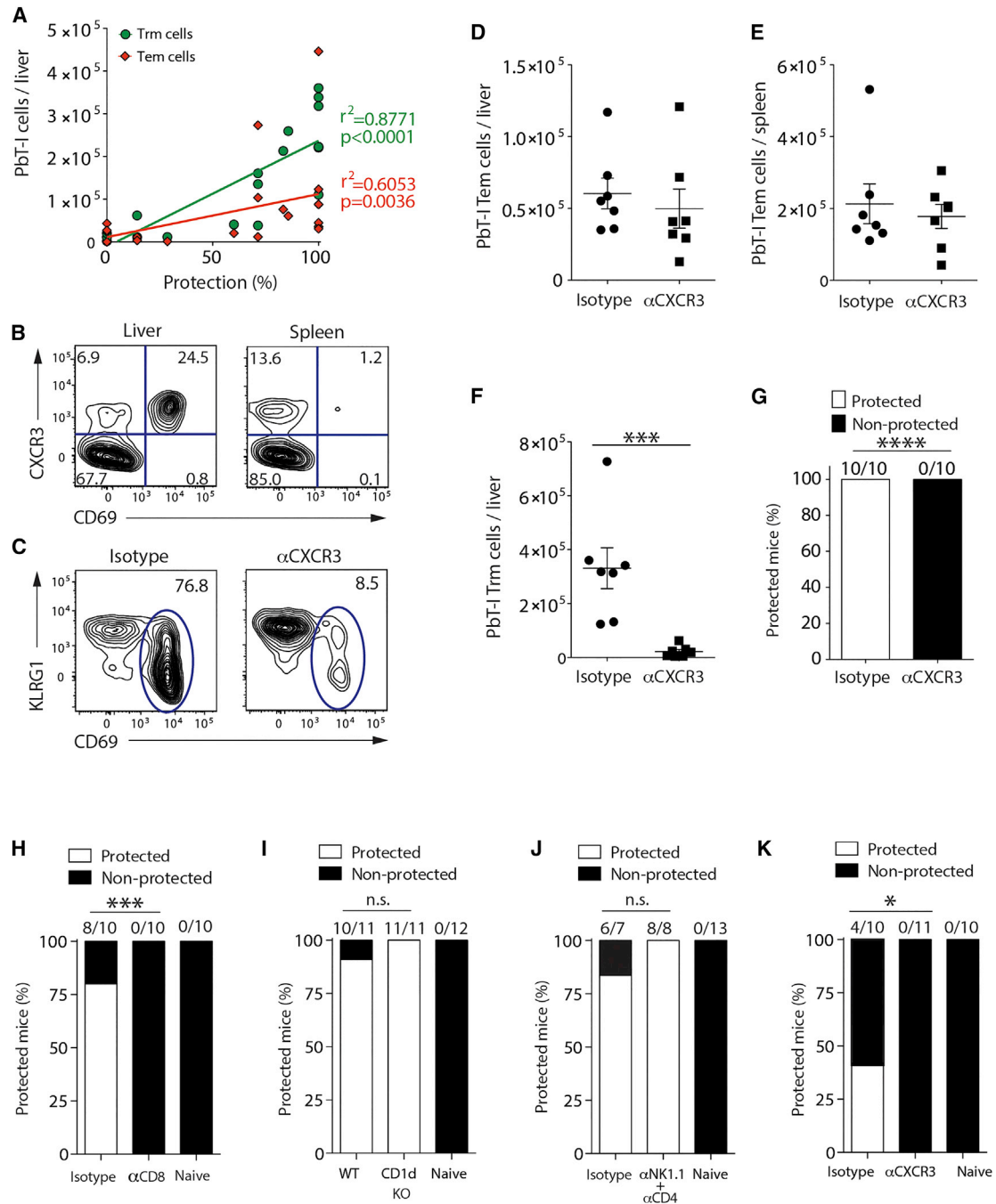


Figure 6. Trm Cells Are Essential for Protection in Prime-and-Trap Vaccinated Mice

(A) Correlation of Trm and Tem cell numbers in the liver with protection in vaccinated mice. Data derived from 13 independent experiments in which mice were adoptively transferred with 50,000 Pbt-I.uGFP cells, then vaccinated with 10B4-NVY combined with either CpG or poly(I:C) 1 day later and, on the next day, either infected with rAAV-NVY virus or left uninfected. Mice were challenged with 200 sporozoites on day 35–64 after priming and protection was assessed by breakthrough parasitemia.

(B) Representative profiles from two independent experiments showing the expression of CXCR3 by Pbt-I cell memory subsets in the liver (left) and spleen (right) on day 23 after vaccination with RAS.

(C–G) Liver Trm cell depletion. B6 mice transferred with Pbt-I cells and vaccinated by prime-and-trap using CpG adjuvant as in Figure 4A were injected with isotype control or α -CXCR3 on days 32 and 34 after vaccination to deplete liver Trm cells. Number of Tem and Trm cells in the liver and spleen were then assessed on day 36 after vaccination.

(C) Representative flow cytometry plots of liver Pbt-I cells showing the proportion of Trm cells in mice that received isotype control Ab (left) or α -CXCR3 Ab (right). Oval gates represent the area where Trm cells (CD69⁺KLRG1^{lo}) were found.

(D and E) Number of Tem cells in the liver (D) and spleen (E) of α -CXCR3 or isotype-treated mice.

(legend continued on next page)

Experimental Procedures. Our first-generation model was based on various estimates and assumptions including (1) Trm cells patrol at 10 μm per min (from Figure 3H), (2) T cell movement can be modeled as a Weiner process (Zaid et al., 2014), (3) the mouse liver is $\sim 1 \text{ cm}^3$ (Melloul et al., 2014), and (4) sinusoids branch about every 50 μm (based on observations from imaging). The liver sinusoidal network was crudely modeled as a three-dimensional cubic lattice with vertices spaced 50 μm apart (Figure 7G) and Trm cells were allowed to move in three dimensions along cube edges, which represent the sinusoids. We estimated the time for a given number of Trm cells to survey a proportion of the liver sinusoid network (Figure 7H). This revealed a substantial ~ 4.5 -fold difference in time to survey 100% of the liver compared to 99%, with only a small additional reduction for 98%. This model estimated that approximately 2.5 million Trm cells were required for 99% coverage within the critical 48 hr window of liver-stage infection. Real values (Figure 6A) suggest that approximately one-tenth this number of Trm cells (as detected by flow cytometry) were 100% protective. Because flow cytometry has been reported to detect only about 20% of T cells in the liver (Steinert et al., 2015), these real numbers approach those predicted in the model for surveillance of 99% of the liver. By refining this model further, we hope to establish the importance of parameters that affect protection, such as Trm cell number, infectious dose, and antigenic properties of the vaccine and parasite.

DISCUSSION

Here we have shown that although various CD8⁺ T cell populations i.e., naive T, Tem, and Tcm cells, can recirculate through the liver, this organ also contains a population of Trm cells. These cells express an array of surface markers, most notably CD69, they lack expression of CD103, and they express increased amounts of the effector molecules granzyme B, IFN- γ , and TNF- α . A previous study also revealed distinct differences between splenic and liver T cell populations after sporozoite vaccination, suggesting that liver T cells expressed a unique transcriptional profile (Tse et al., 2013). Our study largely agreed with this report, with some notable differences. We confirmed differential expression of molecules such as CXCR6, CD69, and CXCR3 by

liver T cells, but distinguished two main populations in the liver, one that expressed these markers and was resident (Trm cells) and one that recirculated and lacked marker expression (Tem cells). In contrast to our study, the earlier report also found a moderate proportion of splenic T cells expressing CD69, CXCR6, and CXCR3. This may relate to their use of *P. yoelii* sporozoites, because this species can provide chronic antigenic stimulation (Cockburn et al., 2010), a property not seen for PbA (Lau et al., 2014). Chronic antigenic stimulation may also explain why the earlier study found increased expression of cell cycle genes in liver Trm cells not seen in our study. One final difference was expression of IL-7R (CD127), which we found elevated in liver Trm over Tem cells whereas the earlier study reported higher expression in the spleen than the liver. This may relate to a greater presence of Tcm cells in the splenic T cell population responding to *P. yoelii*, as this T cell subset expresses high amounts of CD127.

Like liver-resident NKT cells (Thomas et al., 2011), liver Trm cells were found in the sinusoids, where they showed a patrolling phenotype. Such patrolling surveillance has been reported for NKT cells of the liver (Geissmann et al., 2005) and for effector T cells (Guidotti et al., 2015), the latter of which are able to survey hepatocytes for antigen expression by reaching through the fenestrated endothelium of the sinusoids (Guidotti et al., 2015; Warren et al., 2006). In a study of mice vaccinated with a malaria antigen, similar patrolling activity was observed for CD8⁺ T cells in the liver (Cabrera et al., 2013). Although these CD8⁺ T cells were identified only by CD8 expression and additional phenotyping or antigen specificity was not provided, this study highlighted the liver sinusoids as a potential site for parasite surveillance. Adoptive transfer of liver-associated T cells by these authors resulted in cells that failed to patrol, but remained rounded and motionless in the liver, whether recipients were infected or naive. Our observation that liver Trm cells die upon adoptive transfer offers an explanation for these rounded cells, which may be surviving Tem or dying Trm cells. Although parabiotic studies indicated that liver Trm cells remained within their parental livers for several weeks, it is conceivable that even if these intrahepatic cells occasionally entered the broader circulation, their ability to home back to the liver would limit loss long-term. It will be important

(F) Number of Trm cells in the liver of α -CXCR3 or isotype-treated mice.

Data in (D)–(F) were log-transformed and analyzed using an unpaired t test (liver Tem cells, $p = 0.3225$; spleen Tem cells, $p = 0.5571$; liver Trm cells, $p < 0.0001$). Data pooled from three independent experiments. Mean and SEM are shown.

(G–J) Mice were adoptively transferred with naive PbT-I cells, vaccinated by prime-and-trap as in Figure 4A using CpG as adjuvant, and then treated as indicated below before being challenged several weeks later with 200 PbA sporozoites to assess protection. Numbers above bars represent protected mice out of total mice.

(G) Mice depleted of Trm cells are not protected from sporozoite challenge. Immune B6 mice were treated with α -CXCR3 or isotype mAb on days 32 and 34 after vaccination and then challenged day 35 with sporozoites. Data were pooled from two independent experiments (**** $p < 0.0001$, Fisher's exact test).

(H) Mice depleted of CD8⁺ T cells are not protected from sporozoite challenge. Immune B6 mice were injected with 100 μg of isotype control or α -CD8 mAb 1 day before challenge with 200 sporozoites on day 51 or 64 after vaccination. Data pooled from two independent experiments (*** $p < 0.001$, Fisher's exact test).

(I) NKT cells are not required for protection. Immune CD1d-deficient or B6 mice were challenged with 200 sporozoites on day 35 after vaccination. Data pooled from two independent experiments (n.s., $p > 0.05$, Fisher's exact test).

(J) NKT and NK cells are not required for protection. Immune B6 mice were injected with α -NK1.1 (100 μg on days 32, 33, and 34) and α -CD4 (100 μg on days 29 and 33) mAbs or their respective isotype controls, before challenge with 200 sporozoites on day 35. Data pooled from two independent experiments (ns, $p > 0.05$, Fisher's exact test).

(K) Mice vaccinated with RAS and then depleted of liver Trm cells are not protected from sporozoite challenge. B6 mice transferred with PbT-I cells and vaccinated twice with 50,000 RAS 20–21 days apart were injected with 200 μg and 100 μg isotype control or α -CXCR3 mAb on day –3 and day –1 before challenge with 200 sporozoites on day 30–51 after the last vaccination. Data from two independent experiments (* $p = 0.035$, Fisher's exact test).

Please see Movie S7.

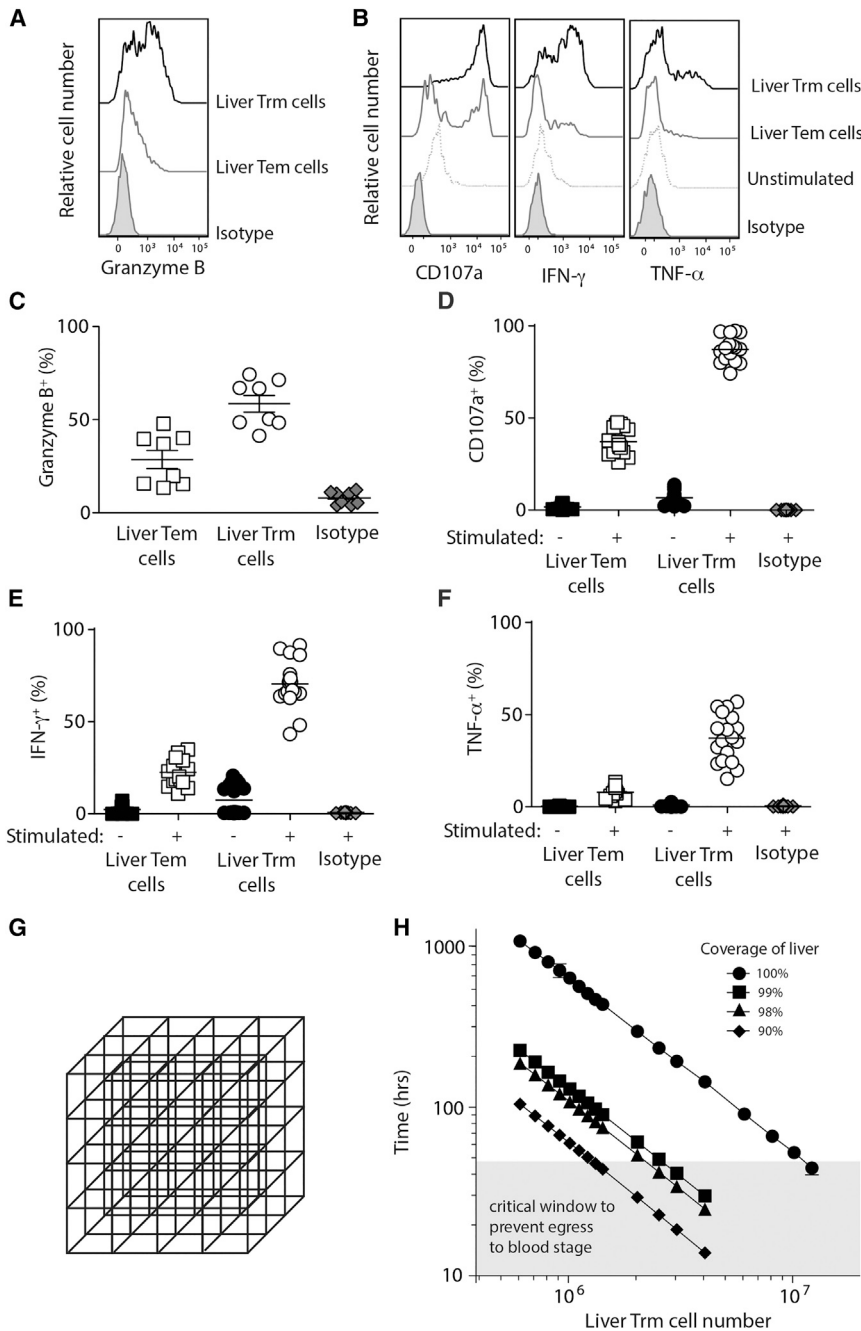


Figure 7. Effector Molecule Expression and Mathematical Modeling of Liver Trm Cells

(A–F) Effector molecule expression by liver Trm and Tem cells. B6 mice were transferred with PbT-1 cells and then vaccinated by prime-and-trap using CpG adjuvant as in Figure 4A. After 34–84 days, mice were injected i.v. with 50 μ g s+16 α -ARTC2.2 nanobody 15 min before harvesting liver T cells. (B, D–F) Liver T cells were restimulated with α -CD3 in vitro for 6 hr before assessing effector molecule expression.

(A and C) Cells were assessed for granzyme B expression without restimulation. (A and B) Representative histograms from two independent experiments.

(C–F) Duplicate samples from each mouse from two independent experiments with lines indicating means and SEM. (G and H) Mathematical modeling of liver surveillance by Trm cells.

(G) Outline of the cubic mesh structure of the mathematical model for liver surveillance as detailed in Supplemental Experimental Procedures. (H) Relationship between number of Trm cells per liver and time for surveillance of a given proportion of this organ (100%, circles; 99%, squares; 98%, triangles; 90%, diamonds). Values represent mean and SD (note: SD were smaller than symbols for most values).

niscient of CD103⁺ Trm cells in the brain, which also require local antigen recognition for their conversion (Wakim et al., 2010). Notably, however, liver Trm cells, like some gut and lymphoid-tissue Trm cells (Bergsbaken and Bevan, 2015; Schenkel and Masopust, 2014), do not express CD103. This may hint at important differences between Trm-like cells in different tissues or simply relate to a lack of CD103-ligand expression in these sites. Although antigen recognition strongly influenced Trm cell formation, the adjuvant used also affected outcome, with CpG being notably more effective than poly(I:C). Signaling through TLR9 has been reported to induce intrahepatic myeloid cell aggregates that enable

to define those receptors that enable liver homing by the treated populations.

Our report suggests that tissue residency need not be purely maintained by location within tissue stroma, as is the case for Trm cells in most tissues, but can be maintained within a blood compartment. This agrees with an earlier study using LCMV-infected mice (Steinert et al., 2015), though this study had not precisely defined the location of liver Trm cells. Our intravital imaging studies show that the vast majority of RAS- and vaccine-induced T cells patrol the sinusoids.

Seeding Trm cells in the liver was best achieved by combining splenic priming with antigen recognition in the liver. This is remi-

CD8⁺ T cell proliferation in the liver (Huang et al., 2013), which raises the possibility that improved formation of Trm cells after CpG administration may relate to a liver-associated inflammatory response, much as inflammation associated with DNFB application to the skin seeded skin Trm cells (Mackay et al., 2012). Although not significant, array analysis showed downregulation of Eomes in liver Trm cells. Downregulation of this transcription factor is important for skin Trm cell development (Mackay et al., 2015) and may be repressed by IL-12, a cytokine induced more efficiently by CpG than poly(I:C).

Recent studies in non-human primates have correlated liver CD8⁺ T cell numbers with protective efficacy after i.v. RAS

vaccination (Ishizuka et al., 2016). Our study showed that large numbers of liver Trm cells correlate with protection. Furthermore, depletion of these cells via CXCR3 abolished protection, questioning a role for the remaining Tem cells. However, whether Tem cells can be recruited by Trm cells, as reported in other organs (Schenkel et al., 2013), to participate in protection is unclear. So far, we have not identified a mAb that can deplete Tem cells alone to measure their contribution.

Our vaccination strategy is a complicated 2-stage approach that is currently impractical for use in the field. However, this proof of concept offers three important advances for next-generation vaccine development. First, it tells us that strategies that maximize liver Trm cell numbers are likely to be of greatest efficacy. Second, it highlights that adjuvant can influence Trm cell formation. And third, it shows that antigen encounter within the liver enhances Trm cell formation. Our future goal is to develop targeting strategies that do not require i.v. vaccine delivery. Antibody-based vaccines, such as α -Clec9A introduced s.c., can readily access the blood and, therefore, i.v. injection is not essential. Evidence that the nature of the adjuvant strongly influences liver Trm cell formation also justifies greater exploration of adjuvant options. Furthermore, Trm cell-based vaccination approaches could be married to vaccines that generate sporozoite-specific humoral immunity, with RTS,S being the obvious option, launching the next generation of more efficacious vaccines.

Our development of a mathematical model for liver surveillance provides a tool that can be further refined to assess important requirements for vaccine design. Knowledge of how Trm cell numbers affect time to survey the liver and the proportion of liver surveyed may determine our choice of antigen type or provide indications as to the value of combining multiple antigens. We can also begin to predict the relationship between the dose of invading sporozoites and the number of Trm cells required to protect. This can help estimate differences in the strength of vaccines required in endemic versus non-endemic areas where the daily dose of sporozoites is likely to vary.

Finally, there are broader implications for the role of Trm cells within the liver. First, these cells may participate positively in responses to viral and bacterial pathogens that infect the liver. Second, their role in infection-related immune pathology of the liver or autoimmune liver diseases needs careful consideration. Susceptibility to depletion via the ARTC2-dependent P2X7 pathway may provide opportunities to limit destructive responses, and blocking this pathway may enhance immunity to pathogens that cause liver damage.

EXPERIMENTAL PROCEDURES

Mice, Mosquitos, Parasites, and Infections

All procedures were performed in strict accordance with the recommendations of the Australian code of practice for the care and use of animals for scientific purposes. The protocols were approved by the Melbourne Health Research Animal Ethics Committee, University of Melbourne (ethic project IDs: 0810527, 0811055, 0911527, 1112347, 1413367, 1513505, 1513639).

C57BL/6 (B6), B6.Ly5.1, GFP, mT/mG, PbT-I, CD1d-deficient, *Cxcr6*-GFP, *Cx3cr1*-GFP, and gBT-I mice were used between 6 and 12 weeks. More details can be found in the [Supplemental Experimental Procedures](#). Animals used for the generation of the sporozoites were 4- to 5-week-old male Swiss Webster mice purchased from the Monash Animal Services (Melbourne, VIC, Australia) and maintained at the School of Botany, The University of Melbourne, Australia.

Anopheles stephensi mosquitoes (strain STE2/MRA-128 from The Malaria Research and Reference Reagent Resource Center) were reared and infected with PbA as described (Benedict, 1997). Sporozoites were dissected from mosquito salivary glands (Ramakrishnan et al., 2013), resuspended in cold PBS, and either left untreated for challenge experiments or irradiated with 20,000 rads using a gamma ⁶⁰Co source. For challenge experiments, 200 freshly dissected PbA sporozoites were injected i.v. as indicated in the figure legend. Blood smears were assessed for parasitemia up to day 12 after infection. Mice showing no evidence of blood-stage infection were assessed as protected.

CD8⁺ T Cell Adoptive Transfer

PbT-I CD8⁺ T cells were negatively enriched from the spleens and lymph nodes of mice from various genetic crosses as described (Smith et al., 2003). 50,000 purified PbT-I cells in 0.2 mL PBS were injected intravenously into recipient mice. For further details see [Supplemental Experimental Procedures](#).

Nanobody-Mediated Blocking of ARTC2.2

Mice were injected i.v. with 50 μ g s+16a nanobody (Rissiek et al., 2014) diluted in 200 μ L PBS and were killed 15 min later. T cells were enriched from the livers and adoptively transferred into naive recipient mice.

Parabiotic Mice

Surgery for generation of parabiotic mice was performed as described (Jiang et al., 2012). For more details see [Supplemental Experimental Procedures](#).

Virus for Vaccination

Recombinant adeno-associated virus (rAAV) was prepared as described previously (Tay et al., 2014). These vectors express membrane-bound ovalbumin bicarbonically with green fluorescent protein (GFP). For the rAAV-OVA vector, this structure was maintained. For the rAAV-NVY vector, the sequence encoding for the natural SIINFEKL epitope of OVA was replaced with the sequence encoding for the PbT-I agonist epitope NVYDNFLL (NVY).

Vaccination

For vaccinations with RAS, B6 mice were injected i.v. with 50,000 RAS. For prime-and-trap experiments, B6 mice were injected i.v. with 8 μ g or 16 μ g of rat α -Clec9A (clone 24/04-10B4) genetically fused to the PbT-I agonist epitope NVY. Anti-Clec9A-NVY (10B4-NVY) was injected with an adjuvant: either 5 nmol of a CpG oligonucleotide (CpG) generated by linking (5' to 3') CpG-2006 to CpG-21798 (Krieg, 2006; Samulowitz et al., 2010) or 50 μ g polyinosinic-polycytidylic acid (poly(I:C)) (Amersham). One day later, mice were infected i.v. with 10⁹ or 10¹⁰ vector gene copies of rAAV expressing NVY or OVA as described.

Statistical Analysis

Figures were generated using GraphPad Prism 5 (GraphPad Software). Data are shown as mean values \pm SEM. Statistical analyses were performed with GraphPad Prism 5, R statistical program, and GSEA software. The statistical test used and p values are indicated in each figure legend. p < 0.05 was considered to indicate statistical significance. *p < 0.05, **p < 0.01, ***p < 0.001, ns, not significant.

Organ processing, flow cytometry, intravital multiphoton microscopy, CD8 T cell exposure to blood, depletion of liver T cells, and assessment of effector function are described in detail in the [Supplemental Experimental Procedures](#).

ACCESSION NUMBERS

The microarray data have been deposited in NCBI GEO database under accession number GSE71518.

SUPPLEMENTAL INFORMATION

Supplemental Information includes four figures, Supplemental Experimental Procedures, one table, and seven movies and can be found with this article online at <http://dx.doi.org/10.1016/j.immuni.2016.08.011>.

AUTHOR CONTRIBUTIONS

D.F.-R., J.Z.M., L.S.L., N.C., D.G.B., F.R.C., J.H.M., B.S.C., M.L., I.A.C., S.N.M., P.B., G.I.M., I.C., and W.R.H. conceived and designed the experiments; D.F.-R., W.Y.N., J.Z.M., A.Z., Y.C.W., L.S.L., N.C., J.L., G.M.D., L.H., A.B., S.S.T., R.S., S.D., Y.K., and M.P. performed experiments; D.F.-R., W.Y.N., J.Z.M., A.Z., G.M.D., R.S., M.P., J.H.M., S.D., Y.K., L.H., S.N.M., I.C., and W.R.H. analyzed the data; and V.M., A.C., D.I.G., P.S.T., F.K.-N., and B.R. provided reagents and gave conceptual advice. W.R.H. wrote the manuscript with D.F.-R., J.Z.M., F.R.C., B.S.C., S.N.M., P.B., and I.C. The research program was led by W.R.H. and I.C., who are senior authors.

ACKNOWLEDGMENTS

We thank members of the F.R.C. and W.R.H. laboratories for discussion and the staff of the Peter Doherty Institute animal facility for animal husbandry. We also thank the Melbourne Brain Centre and ImmunOid Flow Cytometry Facilities for technical assistance. This work was supported by the National Health and Medical Research Council of Australia and the Australian Research Council.

Received: January 26, 2016

Revised: June 21, 2016

Accepted: July 7, 2016

Published: September 27, 2016

REFERENCES

- Benedict, M.Q. (1997). Care and maintenance of anopheline mosquito colonies. In *The Molecular Biology of Insect Disease Vectors*, J.M. Crampton, C. Beard, and C. Louis, eds. (New York: Chapman & Hall), pp. 2–12.
- Berenzon, D., Schwenk, R.J., Letellier, L., Guebre-Xabier, M., Williams, J., and Krzych, U. (2003). Protracted protection to *Plasmodium berghei* malaria is linked to functionally and phenotypically heterogeneous liver memory CD8⁺ T cells. *J. Immunol.* **171**, 2024–2034.
- Bergsbaken, T., and Bevan, M.J. (2015). Proinflammatory microenvironments within the intestine regulate the differentiation of tissue-resident CD8⁺ T cells responding to infection. *Nat. Immunol.* **16**, 406–414.
- Butler, N.S., Vaughan, A.M., Harty, J.T., and Kappe, S.H. (2012). Whole parasite vaccination approaches for prevention of malaria infection. *Trends Immunol.* **33**, 247–254.
- Cabrera, M., Pewe, L.L., Harty, J.T., and Frevort, U. (2013). In vivo CD8⁺ T cell dynamics in the liver of *Plasmodium yoelii* immunized and infected mice. *PLoS ONE* **8**, e70842.
- Cockburn, I.A., Chen, Y.-C., Overstreet, M.G., Lees, J.R., van Rooijen, N., Farber, D.L., and Zavala, F. (2010). Prolonged antigen presentation is required for optimal CD8⁺ T cell responses against malaria liver stage parasites. *PLoS Pathog.* **6**, e1000877.
- Epstein, J.E., Tewari, K., Lyke, K.E., Sim, B.K.L., Billingsley, P.F., Laurens, M.B., Gunasekera, A., Chakravarty, S., James, E.R., Sedegah, M., et al. (2011). Live attenuated malaria vaccine designed to protect through hepatic CD8⁺ T cell immunity. *Science* **334**, 475–480.
- European Medicines Agency (2015). First malaria vaccine receives positive scientific opinion from EMA. Press release. http://www.ema.europa.eu/ema/index.jsp?curl=pages/news_and_events/news/2015/07/news_detail_002376.jsp&mid=W0c0b01ac058004d5c1.
- Galkina, E., Thatte, J., Dabak, V., Williams, M.B., Ley, K., and Braciale, T.J. (2005). Preferential migration of effector CD8⁺ T cells into the interstitium of the normal lung. *J. Clin. Invest.* **115**, 3473–3483.
- Geissmann, F., Cameron, T.O., Sidobre, S., Manlongat, N., Kronenberg, M., Briskin, M.J., Dustin, M.L., and Littman, D.R. (2005). Intravascular immune surveillance by CXCR6⁺ NKT cells patrolling liver sinusoids. *PLoS Biol.* **3**, e113.
- Guidotti, L.G., Inverso, D., Sironi, L., Di Lucia, P., Fioravanti, J., Ganzer, L., Flocchi, A., Vacca, M., Aiolfi, R., Sammiceli, S., et al. (2015). Immunosurveillance of the liver by intravascular effector CD8⁺ T cells. *Cell* **161**, 486–500.
- Huang, L.-R., Wohlbeber, D., Reisinger, F., Jenne, C.N., Cheng, R.-L., Abdullah, Z., Schildberg, F.A., Odenthal, M., Dienes, H.-P., van Rooijen, N., et al. (2013). Intrahepatic myeloid-cell aggregates enable local proliferation of CD8⁺ T cells and successful immunotherapy against chronic viral liver infection. *Nat. Immunol.* **14**, 574–583.
- Ishizuka, A.S., Lyke, K.E., DeZure, A., Berry, A.A., Richie, T.L., Mendoza, F.H., Enama, M.E., Gordon, I.J., Chang, L.J., Sarwar, U.N., et al. (2016). Protection against malaria at 1 year and immune correlates following PfSPZ vaccination. *Nat. Med.* **22**, 614–623.
- Jiang, X., Clark, R.A., Liu, L., Wagers, A.J., Fuhlbrigge, R.C., and Kupper, T.S. (2012). Skin infection generates non-migratory memory CD8⁺ T(RM) cells providing global skin immunity. *Nature* **483**, 227–231.
- Krieg, A.M. (2006). Therapeutic potential of Toll-like receptor 9 activation. *Nat. Rev. Drug Discov.* **5**, 471–484.
- Lahoud, M.H., Ahmet, F., Kitsoulis, S., Wan, S.S., Vremec, D., Lee, C.N., Phipson, B., Shi, W., Smyth, G.K., Lew, A.M., et al. (2011). Targeting antigen to mouse dendritic cells via Clec9A induces potent CD4 T cell responses biased toward a follicular helper phenotype. *J. Immunol.* **187**, 842–850.
- Lau, L.S., Fernandez-Ruiz, D., Mollard, V., Sturm, A., Neller, M.A., Cozijnsen, A., Gregory, J.L., Davey, G.M., Jones, C.M., Lin, Y.-H., et al. (2014). CD8⁺ T cells from a novel T cell receptor transgenic mouse induce liver-stage immunity that can be boosted by blood-stage infection in rodent malaria. *PLoS Pathog.* **10**, e1004135.
- Mackay, L.K., Stock, A.T., Ma, J.Z., Jones, C.M., Kent, S.J., Mueller, S.N., Heath, W.R., Carbone, F.R., and Gebhardt, T. (2012). Long-lived epithelial immunity by tissue-resident memory T (TRM) cells in the absence of persisting local antigen presentation. *Proc. Natl. Acad. Sci. USA* **109**, 7037–7042.
- Mackay, L.K., Rahimpour, A., Ma, J.Z., Collins, N., Stock, A.T., Hafon, M.L., Vega-Ramos, J., Lauzurica, P., Mueller, S.N., Stefanovic, T., et al. (2013). The developmental pathway for CD103^{hi}CD8⁺ tissue-resident memory T cells of skin. *Nat. Immunol.* **14**, 1294–1301.
- Mackay, L.K., Wynne-Jones, E., Freestone, D., Pellicci, D.G., Mielke, L.A., Newman, D.M., Braun, A., Masson, F., Kallies, A., Belz, G.T., and Carbone, F.R. (2015). T-box transcription factors combine with the cytokines TGF- β and IL-15 to control tissue-resident memory T cell fate. *Immunity* **43**, 1101–1111.
- Melloul, E., Raptis, D.A., Boss, A., Pfammater, T., Tschuur, C., Tian, Y., Graf, R., Clavien, P.A., and Lesurtel, M. (2014). Small animal magnetic resonance imaging: an efficient tool to assess liver volume and intrahepatic vascular anatomy. *J. Surg. Res.* **187**, 458–465.
- Nganou-Makamdop, K., van Gemert, G.J., Arens, T., Hermsen, C.C., and Sauerwein, R.W. (2012). Long term protection after immunization with *P. berghei* sporozoites correlates with sustained IFN γ responses of hepatic CD8⁺ memory T cells. *PLoS ONE* **7**, e36508.
- Nussenzweig, R.S., Vanderberg, J., Most, H., and Orton, C. (1967). Protective immunity produced by the injection of x-irradiated sporozoites of *plasmodium berghei*. *Nature* **216**, 160–162.
- Ramakrishnan, C., Delves, M.J., Lal, K., Blagborough, A.M., Butcher, G., Baker, K.W., and Sinden, R.E. (2013). Laboratory maintenance of rodent malaria parasites. *Methods Mol. Biol.* **923**, 51–72.
- Rissiek, B., Danquah, W., Haag, F., and Koch-Nolte, F. (2014). Technical Advance: a new cell preparation strategy that greatly improves the yield of vital and functional Tregs and NKT cells. *J. Leukoc. Biol.* **95**, 543–549.
- Rodrigues, M., Nussenzweig, R.S., and Zavala, F. (1993). The relative contribution of antibodies, CD4⁺ and CD8⁺ T cells to sporozoite-induced protection against malaria. *Immunology* **80**, 1–5.
- RTS,S Clinical Trials Partnership (2014). Efficacy and safety of the RTS,S/AS01 malaria vaccine during 18 months after vaccination: a phase 3 randomized, controlled trial in children and young infants at 11 African sites. *PLoS Med.* **11**, e1001685.
- Samulowitz, U., Weber, M., Weeratna, R., Uhlmann, E., Noll, B., Krieg, A.M., and Vollmer, J. (2010). A novel class of immune-stimulatory CpG oligodeoxynucleotides unifies high potency in type I interferon induction with preferred structural properties. *Oligonucleotides* **20**, 93–101.

- Schenkel, J.M., and Masopust, D. (2014). Tissue-resident memory T cells. *Immunity* *41*, 886–897.
- Schenkel, J.M., Fraser, K.A., Vezyz, V., and Masopust, D. (2013). Sensing and alarm function of resident memory CD8⁺ T cells. *Nat. Immunol.* *14*, 509–513.
- Schmidt, N.W., Podyminogin, R.L., Butler, N.S., Badovinac, V.P., Tucker, B.J., Bahjat, K.S., Lauer, P., Reyes-Sandoval, A., Hutchings, C.L., Moore, A.C., et al. (2008). Memory CD8 T cell responses exceeding a large but definable threshold provide long-term immunity to malaria. *Proc. Natl. Acad. Sci. USA* *105*, 14017–14022.
- Seder, R.A., Chang, L.-J., Enama, M.E., Zephir, K.L., Sarwar, U.N., Gordon, I.J., Holman, L.A., James, E.R., Billingsley, P.F., Gunasekera, A., et al.; VRC 312 Study Team (2013). Protection against malaria by intravenous immunization with a nonreplicating sporozoite vaccine. *Science* *341*, 1359–1365.
- Seman, M., Adriouch, S., Scheuplein, F., Krebs, C., Freese, D., Glowacki, G., Deterre, P., Haag, F., and Koch-Nolte, F. (2003). NAD-induced T cell death: ADP-ribosylation of cell surface proteins by ART2 activates the cytolytic P2X7 purinoceptor. *Immunity* *19*, 571–582.
- Shin, H., and Iwasaki, A. (2012). A vaccine strategy that protects against genital herpes by establishing local memory T cells. *Nature* *491*, 463–467.
- Smith, C.M., Belz, G.T., Wilson, N.S., Villadangos, J.A., Shortman, K., Carbone, F.R., and Heath, W.R. (2003). Cutting edge: conventional CD8 α^+ dendritic cells are preferentially involved in CTL priming after footpad infection with herpes simplex virus-1. *J. Immunol.* *170*, 4437–4440.
- Steinert, E.M., Schenkel, J.M., Fraser, K.A., Beura, L.K., Manlove, L.S., Igyártó, B.Z., Southern, P.J., and Masopust, D. (2015). Quantifying memory CD8 T cells reveals regionalization of immunosurveillance. *Cell* *161*, 737–749.
- Tay, S.S., Wong, Y.C., Roediger, B., Sierro, F., Lu, B., McDonald, D.M., McGuffog, C.M., Meyer, N.J., Alexander, I.E., Parish, I.A., et al. (2014). Intrahepatic activation of naive CD4⁺ T cells by liver-resident phagocytic cells. *J. Immunol.* *193*, 2087–2095.
- Thomas, S.Y., Scanlon, S.T., Griewank, K.G., Constantinides, M.G., Savage, A.K., Barr, K.A., Meng, F., Luster, A.D., and Bendelac, A. (2011). PLZF induces an intravascular surveillance program mediated by long-lived LFA-1-ICAM-1 interactions. *J. Exp. Med.* *208*, 1179–1188.
- Tse, S.-W., Cockburn, I.A., Zhang, H., Scott, A.L., and Zavala, F. (2013). Unique transcriptional profile of liver-resident memory CD8⁺ T cells induced by immunization with malaria sporozoites. *Genes Immun.* *14*, 302–309.
- Tse, S.W., Radtke, A.J., Espinosa, D.A., Cockburn, I.A., and Zavala, F. (2014). The chemokine receptor CXCR6 is required for the maintenance of liver memory CD8⁺ T cells specific for infectious pathogens. *J. Infect. Dis.* *210*, 1508–1516.
- Wakim, L.M., Woodward-Davis, A., and Bevan, M.J. (2010). Memory T cells persisting within the brain after local infection show functional adaptations to their tissue of residence. *Proc. Natl. Acad. Sci. USA* *107*, 17872–17879.
- Warren, A., Le Couteur, D.G., Fraser, R., Bowen, D.G., McCaughan, G.W., and Bertolino, P. (2006). T lymphocytes interact with hepatocytes through fenestrations in murine liver sinusoidal endothelial cells. *Hepatology* *44*, 1182–1190.
- Weiss, W.R., Sedegah, M., Beaudoin, R.L., Miller, L.H., and Good, M.F. (1988). CD8⁺ T cells (cytotoxic/suppressors) are required for protection in mice immunized with malaria sporozoites. *Proc. Natl. Acad. Sci. USA* *85*, 573–576.
- Zaid, A., Mackay, L.K., Rahimpour, A., Braun, A., Veldhoen, M., Carbone, F.R., Manton, J.H., Heath, W.R., and Mueller, S.N. (2014). Persistence of skin-resident memory T cells within an epidermal niche. *Proc. Natl. Acad. Sci. USA* *111*, 5307–5312.